OXYGEN TRANSPORT THROUGH DENSE PEROVSKITE-TYPE $La_{1-x}Sr_xFeO_{3-\delta}$ MEMBRANES

J.E. ten Elshof, H.J.M. Bouwmeester and H. Verweij

University of Twente, Laboratory of Inorganic Materials Science,
P.O. Box 217, 7500 AE Enschede, the Netherlands

Oxygen permeation measurements were performed on dense $La_{1-x}Sr_xFeO_{3-\delta}$ (x=0.1-0.4) membranes at 1273 K. The materials were investigated in air/He and air/He,CO,CO_2 gradients. The fluxes increased with increasing Sr content and were strongly enhanced by the presence of CO, up to values of 25 mmol m^{-2} s^{-1}. In air/He gradients the permeation is bulk controlled and can be modelled by Wagner theory incorporating a random point defect model. Oxygen vacancy diffusion coefficients were calculated to range between $5.6\text{-}8.6\cdot10^{-6}$ cm^2 s^{-1}. In air/CO,CO_2 gradients the permeation process appeared to be totally limited by the surface reaction rate. To account for this behaviour, models are proposed in which surface oxygen vacancies act as active surface sites.

INTRODUCTION

The oxygen permeation properties of dense perovskite-type membranes are receiving considerable scientific attention recently, due to their possible application as oxygen separation membrane for the production of oxygen [1,2] or for direct supply of oxygen into chemical reactors, *e.g.* in the upgrading of natural gas [3,4]. Since oxygen transport can only take place through the crystal lattice by hopping of oxygen anions to neighbouring vacant sites, the transport of any other species is excluded, so that dense membranes have an infinite permselectivity.

The electronic and ionic conductivities, oxygen vacancy concentrations, *etc.*, of perovskites are strongly dependent on the ambient conditions. There are indications that ordering or clustering of oxygen vacancies can occur [5], which will influence the transport negatively, since ordered oxygen vacancies are considered to be immobile.

The relationship between the defect chemistry and the oxygen permeation behaviour of $La_{1-x}Sr_xFeO_{3-\delta}$ (LSF) membranes is the aim of the present work. The defect chemistry of LSF as a function of temperature, oxygen partial pressure and Sr content is well understood [6], which makes it an attractive material for modelling purposes. In comparison with LSF, cobaltite perovskites $La_{1-x}Sr_xCoO_{3-\delta}$ show higher oxygen fluxes under comparable circumstances [2]. However, LSF has a much larger chemical stability in reducing atmospheres, which is considered to be of importance for application in membrane reactors.

A further issue of both practical [3] and theoretical concern is the question whether the oxygen flux is limited by bulk diffusion or by a surface exchange process occurring at one of the gas/solid interfaces. The transition from bulk to surface limitation occurs typically when the thickness of the membrane is of the order of D^*/k, where D^* ($cm^2\ s^{-1}$) is the tracer diffusion coefficient, and k ($cm\ s^{-1}$) is the surface exchange coefficient. As follows from data of isotopic exchange [7], the thicknesses for LSF (x=0.1-0.4) can be estimated to fall in the range 0.06-0.45 mm at 1273 K and 0.065 bar O_2. In this paper, we report a study on the permeation behaviour of LSF membranes (x=0.1-0.4) in small and large oxygen activity gradients. The observations are discussed in relation with the defect chemistry exhibited by these materials.

THEORY

Bulk diffusion

Diffusion of oxygen species through dense perovskite membranes is generally described within the framework of the Wagner theory [8]:

$$j_{O_2} = \frac{RT}{4^2F^2L}\int_{p_{O_2}''}^{p_{O_2}'} \frac{\sigma_{O^{2-}}\sigma_{el}}{\sigma_{O^{2-}}+\sigma_{el}}\, d\ln p_{O_2} \tag{1}$$

In Eq. (1), j_{O2} is the oxygen permeation flux in mol $m^{-2}\ s^{-1}$, p_{O2}' and p_{O2}'' are the oxygen partial pressures at opposite sides of the membrane, and L is the membrane thickness (m). σ_{O2-} and σ_{el} refer to the ionic and electronic conductivities, respectively ($S\ m^{-1}$). F is Faraday's constant. At oxygen partial pressures above 10^{-7} bar, the electronic conductivity in LSF is several orders of magnitude larger than the ionic conductivity, so that

$$j_{O_2} = \frac{RT}{4^2F^2L}\int_{p_{O_2}''}^{p_{O_2}'} \sigma_{O^{2-}}\, d\ln p_{O_2} \tag{2}$$

For the ionic conductivity, we use the Nernst-Einstein relation in a form

$$\sigma_{O^{2-}} = \frac{4F^2D_V\delta}{RTV_m} \tag{3}$$

with D_V, δ and V_m the oxygen vacancy diffusion coefficient ($m^2\ s^{-1}$), oxygen vacancy concentration and molar volume of perovskite ($m^3\ mol^{-1}$), respectively. The dependence of the oxygen vacancy diffusion coefficient on oxygen stoichiometry is taken into account, considering the fact that an oxygen vacancy can only jump to an occupied neighbouring site, the fraction of which equals (1-δ/3). Thus, a stoichiometry-renormalized vacancy diffusion coefficient D_V^0 may be defined as

$$D_V = D_V^0\left(1 - \frac{\delta}{3}\right) \tag{4}$$

Values of D_V for x=0.1-0.4 were reported by Ishigaki *et al.* [7] from data of $^{18}O/^{16}O$ isotope exchange. It was suggested that D_V is virtually independent of the Sr content.

The ionic conductivity can also be written empirically as

$$\sigma_{O^{2-}} = \sigma_0 p_{O_2}^{n(p_{O_2})} \tag{5}$$

where σ_0 (S m^{-1}) is a constant and n is called the order.

When a detailed defect model is available for the composition under consideration, n can be calculated for a given temperature and oxygen pressure from

$$n(p'_{O_2}) = \left(\frac{\partial \ln \sigma_{O^{2-}}(p'_{O_2})}{\partial \ln p'_{O_2}}\right) = \left(\frac{\partial \ln D_V \delta}{\partial \ln p'_{O_2}}\right) \approx \left(\frac{\partial \ln \delta}{\partial \ln p'_{O_2}}\right) \tag{6}$$

Since D_V remains essentially constant upon changing oxygen pressure, n will be determined mainly by the change of δ.

Extensive TG analyses on LSF materials were performed by Mizusaki *et al.* [6]. The investigated temperature and oxygen pressure ranges were 873-1473 K and 10^{-20}-1 bar, respectively, while the Sr dopant concentration x was varied between 0 and 0.6. All results could be explained in terms of a simple point defect model, assuming a random distribution of defect species. In Kröger-Vink notation [9], this defect model can be described by two defect reactions as:

$$2Fe_{Fe}^{x} + V_O^{\cdot\cdot} + 1/2\,O_2(g) \rightleftharpoons 2Fe_{Fe}^{\cdot} + O_O^{x} \tag{7}$$

$$2Fe_{Fe}^{x} \rightleftharpoons Fe_{Fe}^{\cdot} + Fe_{Fe}^{\prime} \tag{8}$$

With the equilibrium constants for these reactions and the condition of overall charge neutrality, the concentrations of all defect species can be calculated for a given x, p_{O_2} and T [6]. The oxygen contents of phases LSF at 1273 K are illustrated in Figure 1.

Surprisingly, the pre-exponential factors and activation energies of the equilibrium constants are almost independent of the strontium content [6]. Moreover, the equilibrium constants are also essentially independent of the level of nonstoichiometry, even at high δ. This implies that even at high oxygen vacancy concentrations, no interaction occurs between the ionic defects. This may be explained by screening due to a high electronic conductivity of small polarons. However, such an explanation does not hold for compounds $La_{1-x}Sr_xCoO_{3-\delta}$ [10], which show metallic conductivity at elevated temperatures.

Surface exchange processes

In the absence of a chemical reaction occurring at one of the gas/solid interfaces, the overall reactions for the incorporation and release of oxygen can be written as

$$\tfrac{1}{2}O_2 \rightleftharpoons O_O^x + 2h^{\cdot} \tag{9}$$

Ishigaki *et al.* [7] determined the surface exchange coefficients in chemical equilibrium for x=0.1-0.4, but no details are known about the exchange mechanism. Boukamp *et al.* [11] proposed a 2-step mechanism to model data of $^{18}O/^{16}O$ exchange on fluorite-type $Bi_{1.5}Er_{0.5}O_3$:

$$O_2 + 2S_V + 2e' \rightleftharpoons 2O_{ad}^- \tag{10}$$

$$2O_{ad}^- + 2e' + 2V_O^{\cdot\cdot} \rightleftharpoons 2O_O^x + 2S_V \tag{11}$$

S_V is a surface site on which oxygen can adsorb. It was found that the first step limits the overall oxygen flux. More recently, Kilner suggested that oxygen surface oxygen vacancies may play an active role in oxygen exchange [12].

When a chemical reaction occurs at one of the sides of the membrane, the oxygen permeation flux may become influenced. A low oxygen activity at one of the membrane sides can be achieved by using CO/CO_2 mixtures. However, this will also change the mechanism of the surface reaction [13]. Oxygen permeated through the membrane will react with CO to CO_2 according to

$$CO + O_O^x + 2h^{\cdot} \rightarrow CO_2 + V_O^{\cdot\cdot} \tag{12}$$

Since the reaction $CO+\frac{1}{2}O_2 \rightleftharpoons CO_2$ in the gas phase reaches equilibrium quickly, the oxygen activity at the low partial pressure side of the membrane is well-defined when ideal mixing behaviour is assumed.

EXPERIMENTAL

Compositions LSF with Sr contents x=0.1-0.4 were made by the citrate synthesis from standardized solutions of the nitrates of the constituent metals. The powders were calcined at 1123-1150 K for 10 h and ball-milled with YSZ milling balls in acetone for 3 h. Disks of 20 mm diameter were made by uniaxial pressing at 1.5 bar and isostatic pressing at 4000 bar. Sintering was performed at 1473 K for 18-24 h in air. Membranes of 12.0 mm diameter and thicknesses 0.5-2.0 mm were cut from the sintered disks and polished with SiC (1000 MESH). The thicknesses of the membranes were determined within 0.02 mm. The phase purity and lattice parameters were determined with XRD.

The measurements were performed in a quartz reactor. Details can be found elsewhere [14]. He or $He/CO/CO_2$ mixtures were fed to the permeate side of the membrane, while an O_2/N_2 mixture (p_{O_2} ranging from 10^{-2}-1 bar) was supplied to the feed side. The oxygen partial pressures of the permeate and retentate streams were continuously monitored by oxygen sensors. Analysis of the permeate side gas mixture was done by GC detection.

The membranes were sealed to the reactor by glass rings at 1310-1330 K. Due to this sealing procedure the geometric surface area exposed to the low oxygen partial pressure side is smaller than the area exposed to the higher oxygen pressure. As a result, diffusion through the membrane is not purely one-dimensional; there is also a non-axial contribution to the total flux. In the absence of CO/CO_2 mixtures, the oxygen fluxes were calculated from

$$j_{O_2} = \frac{1}{G} \cdot \frac{F p_{O_2}}{RTA} \tag{13}$$

where F is the flow rate of the permeate stream ($m^3\ s^{-1}$), p_{O_2} the oxygen partial pressure in the effluent stream ($N\ m^{-2}$), A the geometric surface area at the permeate side (m^2), and G a dimensionless factor correcting for the effect of non-axial diffusion. Details concerning the calculation of G can be found elsewhere [15].

When CO and CO_2 were present, the flux was calculated from the mass balance according to

$$j_{O_2} = \frac{F}{RTA}\left(p_{CO_2}^{out} - p_{CO_2}^{in} + \frac{1}{2}\left(p_{CO}^{out} - p_{CO}^{in}\right)\right) \tag{14}$$

in which p_i^{in} and p_i^{out} are the inlet and outlet pressures of species i ($N\ m^{-2}$). The gas tightness of membrane/seal was checked by GC detection of N_2 in the effluent stream. The contribution of leaked oxygen to the total flux was less than 1% for all data reported here.

RESULTS

Permeation in air/He gradients

Oxygen permeation fluxes on 1 mm thick membranes are given versus time in Figure 2. Although $La_{0.6}Sr_{0.4}FeO_{3-\delta}$ appears to reach a steady state flux relatively fast, *i.e.* within 30 h, the compositions x=0.1-0.3 equilibrate much slower in similar gradients. The influence of a 2 h exposure of the lean-side of a $La_{0.8}Sr_{0.2}FeO_{3-\delta}$ membrane to a CO/CO_2 atmosphere (p_{CO}=p_{CO_2}=0.2 bar) is illustrated. Surprisingly, equilibration is fast after exposure. Similar observations were made for other compositions. Possibly, the surface is modifiied upon exposure to CO. All further results reported here refer to measurements after treatment.

Thickness dependence measurements are shown in Figure 3 for x=0.1 and x=0.4. It is seen that the oxygen fluxes are inversely proportional to the membrane thickness, in agreement with Eq. (2). Thus, CO treatment of the lean-side enhances the surface process to such extent that a limitation by bulk diffusion occurs.

To verify whether the oxygen flux can be understood in terms of the random point defect model, its oxygen partial pressure dependence was measured for each of the compositions. The effect of the feed side oxygen pressure is given in Figure 4. The order n_{expt} was determined by fitting the fluxes to the empirical equation

$$j_{O_2} = \alpha p_{O_2}^{n_{expt}} + \beta \quad (15)$$

If the nonstoichiometry model holds, the value of n_{expt} should be close to the value of $\langle n \rangle$ that can be calculated by averaging of $n(p_{O_2})$ (Eq. (6)) over the investigated partial pressure range. The corresponding values are compared in Table 1. The close agreement observed between n_{expt} and $\langle n \rangle$ suggests the validity of the point defect model. Given these results, we may conclude that the oxygen fluxes can be described properly by Eqs. (2) and (3). The molar volumes V_m were calculated from XRD measurements at room temperature, although the assumption made that the lattice parameters are not influenced by temperature and oxygen partial pressure does not hold entirely [4]. The D_V^0 values can then be determined by fitting of Eq. (3) to the experimental fluxes. The results are given in Table 2 and are compared with the results from the $^{18}O/^{16}O$ exchange study by Ishigaki *et al.* [7] in Figure 5. Although Ishigaki *et al.* found a small dependence of the Sr content on the vacancy diffusion coefficient, the D_V^0 values obtained in this study are essentially independent of x.

Permeation in air/CO,CO$_2$ gradients

When the same membrane systems are placed in a large oxygen activity gradient, the observed oxygen fluxes can no longer be described in terms of bulk diffusion limited behaviour, although the presence of CO strongly enhances oxygen permeation in comparison with the results from measurements in air/He. No correlation was seen between the oxygen activity at the lean side of the membrane and the oxygen flux. Furthermore, no thickness dependence was observed, while a linear relation was observed between the CO partial pressure and j_{O_2}, as shown in Figure 6. The absence of mass transport limitations was confirmed by flow dependent measurements. The observed oxygen fluxes did not change upon lowering the feed side oxygen partial pressure from 1 to $10^{-1.7}$ bar. It is therefore concluded that the permeation process under the conditions covered by the experiments is fully limited by the oxidation process occurring at the surface.

When the slopes of the curves of Figure 6 are plotted versus the Sr content, as shown in Figure 7, a second linear relationship is seen. These observations may be accounted for by considering that the oxygen partial pressures at the CO side all fall within the plateau regions of the nonstoichiometry (Figure 1), where $\delta \approx \frac{1}{2}x$. Thus, the nonstoichiometries are proportional to the Sr content under these conditions.

We may account for both observed linear dependencies in terms of an Eley-Rideal type of mechanism [16] by assuming that a surface oxygen anion becomes susceptible to attack by CO only when it is residing next to a surface oxygen vacancy:

$$CO + O_O^x\text{-}V_O^{\cdot\cdot} \rightarrow CO_2 + V_O^{\cdot\cdot}\text{-}V_O^{\cdot\cdot} + 2e'$$

At low oxygen vacancy concentrations, the observed flux will be proportional to δ, *i.e.* $[O_O^x\text{-}V_O^{\cdot\cdot}] \sim \delta$. The maximum nonstoichiometry reached here is about 0.15 for x=0.3, which equals 5% of the total oxygen content.

An alternative explanation may be given in terms of a Langmuir-Hinshelwood type of

mechanism [16], in which CO adsorbs to a surface oxygen vacancy prior to reaction with an oxygen anion:

$$CO + V_O^{\cdot\cdot} \rightarrow \left\langle V_O^{\cdot\cdot}\text{-}CO \right\rangle^{\cdot} \tag{17}$$

$$\left\langle V_O^{\cdot\cdot}\text{-}CO \right\rangle^{\cdot} + O_O^{x} \rightarrow CO_2 + 2V_O^{\cdot\cdot} + 2e' \tag{18}$$

If it is further assumed that the adsorption of CO is the rate-limiting step in the overall oxygen permeation process, the oxygen flux may be expressed by

$$j_{O_2} = \tfrac{1}{2} k_0 \delta p_{CO} \tag{19}$$

where k_0 is a constant independent of composition. Eq. (18) fully accounts for the observations made above.

The involvement of surface oxygen vacancies in the surface exchange process has also been concluded from electrical conductivity relaxation measurements in CO/CO_2 atmospheres on $La_{1-x}Ca_xCrO_{3-\delta}$ [17], where a roughly proportional relationship was established between the surface exchange coefficient and the nonstoichiometry.

CONCLUSIONS

Oxygen permeation measurements on LSF membranes with Sr contents of 10-40% were performed in air/He and air/He,CO,CO_2 gradients at 1273 K. In air/He gradients, the oxygen permeation is limited by the diffusion of oxygen through the bulk of the material. The observed fluxes are in the range of $0.1\text{-}4.5 \cdot 10^{-7}$ mmol m^{-2} s^{-1}, being a function of the Sr content. The fluxes can be modelled by Wagner theory in conjunction with a point defect model for the nonstoichiometry. By adjusting the values of the oxygen vacancy diffusion coefficients D_V^0 to the observed fluxes, it was found that D_V^0 is hardly influenced by the Sr content.

Upon placing the same materials in large gradients, *i.e.* air/CO,CO_2, the permeation process becomes fully limited by the oxidation rate of CO at the permeate side of the membrane. A simple mechanism for the oxidation process is proposed to account for these observations. It is assumed that surface oxygen vacancies behave as adsorption sites for CO. This adsorption step is also believed to be rate-limiting the oxygen permeation.

ACKNOWLEDGEMENTS

The support of the Commission of the European Communities in the framework of the Joule programme, sub-programme Energy from Fossil Resources, Hydrocarbons, is gratefully acknowledged.

REFERENCES

1. L. Qiu, T.H. Lee, L.-M. Liu, Y.L. Yang, and A.J. Jacobson, Solid State Ionics, **76** 321 (1995).
2. N. Itoh, T. Kato, K. Uchida, and K. Haraya, J. Membr. Sci., **92** 239 (1994).
3. J.E. ten Elshof, H.J.M. Bouwmeester, and H. Verweij, Appl. Catal. A, in press (1995).
4. S. Pei, M.S. Kleefisch, T.P. Kobylinski, J. Faber, C. Udovich, V. Zhang-McCoy, B. Dabrowski, U. Balachandran, R.L. Mieville, and R.B. Poeppel, Catal. Let., **30** 201 (1995).
5. H. Kruidhof, H.J.M. Bouwmeester, R.H.E. van Doorn, and A.J. Burggraaf, Solid State Ionics, **63-65** 816 (1993).
6. J. Mizusaki, M. Yoshihiro, S. Yamauchi, and K. Fueki, J. Solid State Chem., **58** 257 (1985).
7. T. Ishigaki, S. Yamauchi, K. Kishio, J. Mizusaki, and K. Fueki, J. Solid State Chem., **73** 179 (1985).
8. C. Wagner, Z. Phys. Chem., **21** 25 (1933).
9. F.A. Kröger, The chemistry of imperfect crystals, North-Holland, Amsterdam, 1964.
10. J. Mizusaki, Y. Mima, S. Yamauchi, K. Fueki, and H. Tagawa, J. Solid State Chem., **80** 102 (1989).
11. B.A. Boukamp, H.J.M. Bouwmeester, and A.J. Burggraaf, Proc. 2nd Intl. Symp. on Ionic and Mixed Conducting Oxides, T.A. Ramanarayanan, W.L. Worrell, and H.L. Tuller (Eds), 141 (1994).
12. J.A. Kilner, Proc. 2nd Intl. Symp. on Ionic and Mixed Conducting Oxides, T.A. Ramanarayanan, W.L. Worrell, and H.L. Tuller (Eds), 174 (1994).
13. E.Kh. Kurumchin, and M.V. Perfiliev, Solid State Ionics, **42** 129 (1990).
14. B.A. van Hassel, J.E. ten Elshof, and H. Verweij, Appl. Catal. A, **119** 279 (1994).
15. J.E. ten Elshof, H.J.M. Bouwmeester, and H. Verweij, Solid State Ionics, accepted (1995).
16. J.A. Moulijn, P.W.N.M. van Leeuwen, and R.A. van Santen (Eds), Catalysis: An integrated approach to homogeneous, heterogeneous and industrial catalysis, Elsevier, Amsterdam, 1993.
17. I. Yasuda and T. Hikita, J. Electrochem. Soc., **141** 1268 (1994).

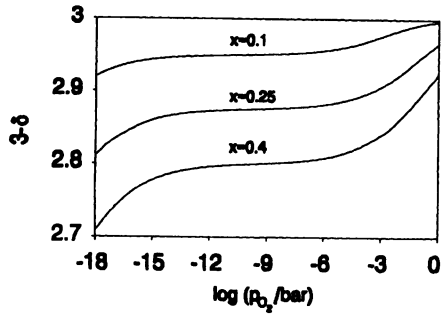

Figure 1 Oxygen content of LSF phases x=0.1, 0.25 and 0.4 at 1273 K versus oxygen partial pressure.

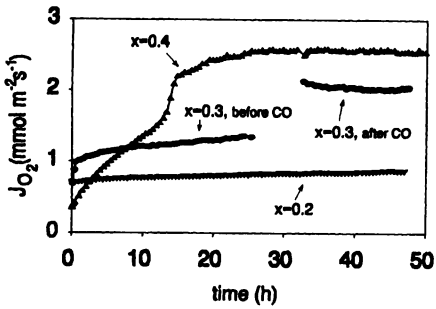

Figure 2 Oxygen flux through 1 mm thick membranes at 1273 K (x=0.2-0.4) versus time after sealing.

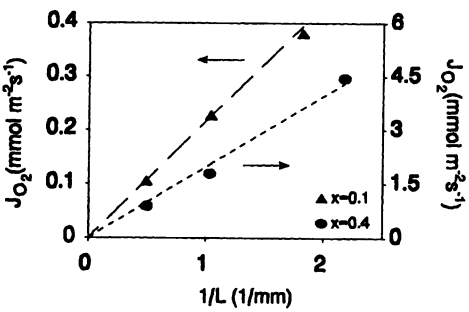

Figure 3 Dependence of membrane thickness on oxygen flux for LSF (x=0.1-0.4) at 1273 K.

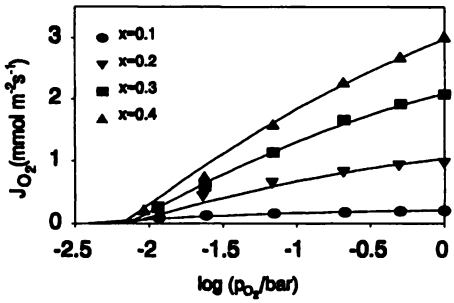

Figure 4 Comparison between experimental oxygen fluxes and model calculations through 1 mm membranes (x=0.1-0.4) at 1273 K.

x	n_{expt}	$\langle n \rangle$
0.1	-0.39	-0.42
0.2	-0.24	-0.20
0.3	-0.17	-0.16
0.4	-0.09	-0.12

Table 1 Experimental and theroretical orders of the oxygen pressure with respect to the oxygen flux at 1273 K.

x	D_V^0 (10^{-6} cm^2 s^{-1})
0.1	5.65
0.2	7.71
0.3	8.06
0.4	8.56

Table 2 Vacancy diffusion coefficients at 1273 K.

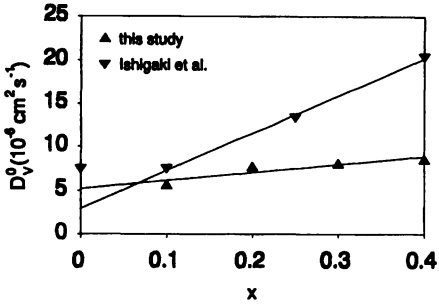

Figure 5 Comparison of vacancy diffusion coefficients.

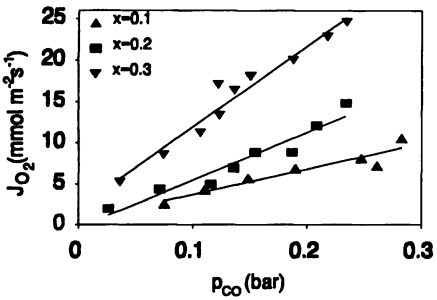

Figure 6 Oxygen fluxes through LSF membranes (x=0.1-0.3) versus the CO partial pressure at 1273 K.

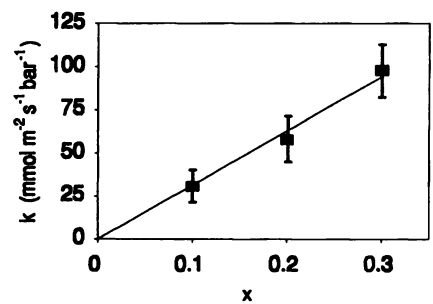

Figure 7 Slopes of plots in Figure 6 versus Sr content.